MNRAS 000, 1–6 (2016) Preprint 1 February 2017 Compiled using MNRAS LaTeX style file v3.0

Increasing Fisher Information by Moving-Mesh Reconstruction

Qiaoyin Pan[1,2⋆], Ue-Li Pen[2,3,4,5†], Derek Inman[2,6], Hao-Ran Yu[2,7]

[1] *School of Physics, Nankai University, 94 Weijin Rd, Nankai, Tianjin, 300071, China*
[2] *Canadian Institute for Theoretical Astrophysics, University of Toronto, 60 St. George Street, Toronto, Ontario M5S 3H8, Canada*
[3] *Dunlap Institute for Astronomy and Astrophysics, University of Toronto, Toronto, ON M5S 3H4, Canada*
[4] *Canadian Institute for Advanced Research, Program in Cosmology and Gravitation*
[5] *Perimeter Institute for Theoretical Physics, Waterloo, ON, N2L 2Y5, Canada*
[6] *Department of Physics, University of Toronto, 60 St. George, Toronto, ON M5S 1A7, Canada*
[7] *Kavli Institute for Astronomy and Astrophysics, Peking University, Beijing 100871, China*

1 February 2017

ABSTRACT

Reconstruction techniques are commonly used in cosmology to reduce complicated nonlinear behaviours to a more tractable linearized system. We study a new reconstruction technique that uses the Moving-Mesh algorithm to estimate the displacement field from nonlinear matter distribution. We show the performance of this new technique by quantifying its ability to reconstruct linear modes. We study the cumulative Fisher information $I(< k_n)$ about the initial matter power spectrum in the matter power spectra in 130 N-body simulations before and after reconstruction, and find that the nonlinear plateau of $I(< k_n)$ is increased by a factor of ~ 50 after reconstruction, from $I \simeq 2.5 \times 10^{-5}/(\mathrm{Mpc}/h)^3$ to $I \simeq 1.3 \times 10^{-3}/(\mathrm{Mpc}/h)^3$ at large k. This result includes the decorrelation between initial and final fields, which has been neglected in some previous studies. We expect this technique to be beneficial to problems such as baryonic acoustic oscillations, redshift space distortions and cosmic neutrinos that rely on accurately disentangling nonlinear evolution from underlying linear effects.

Key words: cosmology: theory — large-scale structure of Universe.

1 INTRODUCTION

Two-point statistics provide complete descriptions of Gaussian density fields and can be computed efficiently even for large data sets. However, nonlinear gravitational evolution leads to highly non-Gaussian matter distributions which require higher order statistics to fully characterize. Such statistics are computationally expensive and can be challenging to map to cosmological parameters. To mitigate these difficulties, it is common to transform the matter field in a way that hopefully reduces non-Gaussianity. For example, Gaussianization transforms have been used to make the logarithmic distribution more Gaussian (Weinberg 1992; Neyrinck et al. 2009) and wavelet nonlinear Wiener filters have been used to separate Gaussian and non-Gaussian components of the density field (Zhang et al. 2011; Yu et al. 2012; Harnois-Déraps et al. 2013b). *Reconstruction* techniques (Eisenstein et al. 2007a) provide a more effective way by converting matter distributions back to an earlier stage (Harnois-Déraps et al. 2013b).

The quality of these techniques can be quantified by computing the Fisher information (Rimes & Hamilton 2005) present in the power spectrum before and after reconstruction/Gaussianization. Meiksin & White (1999) were the first to study the Fisher information in the nonlinear matter power spectrum calculated from N-body simulations. They found that the cumulative information has a plateau on translinear scales ($k \simeq 0.2 - 0.8$ h/Mpc) due to strong coupling between Fourier modes. Qualitatively, this means that the power spectra on these scales give little additional information. Ngan et al. (2012) applied the linear reconstruction using the Zel'dovich approximation on nonlinear density fields, and found that the cumulative Fisher information increases slightly. Harnois-Déraps et al. (2013b) computed the cumulative Fisher information for various Gaussianization methods and their combinations and found that while mode coupling is reduced, there is not necessarily an improvement in the cross correlation between the initial density fields and the final nonlinear ones.

In studies of Baryon Acoustic Oscillations (BAO), density fields are subjected to reconstruction which partially inverts nonlinear evolution by applying the negative Zel'dovich

⋆ panda@mail.nankai.edu.cn
† pen@cita.utoronto.ca

displacement field (Eisenstein et al. 2007b; Zel'dovich 1970). Yu et al. (2016) studied the curl-free, or E-mode, component of the exact displacement field in Lagrangian space and found that the linear density field can be well recovered by the E-mode displacement field. This E-mode reconstruction therefore provides a theoretical target for other reconstruction techniques to be compared with. Recently Zhu et al. (2016a,b) described a new reconstruction technique using the Moving-Mesh algorithm (MM), first described in (Pen 1995, 1998), to effectively estimate $\mathbf{\Psi}(\boldsymbol{q})$ from only nonlinear density fields. They further showed that even though shell-crossing and vorticity are not recovered, linear density modes are still recovered up to scales relevent to the BAO.

In this paper, we compute the Fisher information recovered after using this new reconstruction scheme on 130 independent N-body simulations, and compared with other methods and unreconstructed fields. The paper is organized as follows. In §2, we briefly describe the computation of the displacement potential using MM algorithm. In §3, we describe the simulations, implementation of the reconstruction and compare the power spectra and cross correlations before and after reconstruction. In §4, we further compute the correlation matrix and Fisher information before and after reconstruction. Finally, in §5, we summarize our results and discuss the effectiveness of the reconstruction.

2 RECONSTRUCTION TECHNIQUE

Here we briefly review the MM algorithm used in the new reconstruction technique; for a more complete description we refer the reader to Zhu et al. 2016b. The aim of the MM algorithm is to estimate the displacement field of mass elements in Lagrangian coordinates from their final Eulerian position only, and from this estimated displacement field one directly reconstructs the linear density field. The general principle is to relate the Eulerian coordinates of a mass element, x^i, to a curvilinear system, ξ^μ, such that the mass per grid cell is approximately constant,

$$\rho\sqrt{g} = \text{Const.}, \tag{1}$$

where $\sqrt{g} \equiv \det\left|e^i_\mu\right|$ is the volume element and $e^i_\mu \equiv \partial x^i/\partial\xi^\mu$ is the coordinate transformation matrix. These coordinates are related via a *deformation* field, which we assume to be a pure gradient:

$$x^i = \xi^\mu \delta^i_\mu + \frac{\partial\phi}{\partial\xi^\mu}\delta^{i\mu}, \tag{2}$$

and ϕ is called the *deformation potential* which is chosen to satisfy Eq. 1.

Numerically, we iteratively solve for the deformation potential via a diffusion equation,

$$\partial_\mu(\rho\sqrt{g}e^\mu_i\delta^{i\nu}\partial_\nu\dot{\phi}) = \Delta\rho, \tag{3}$$

where $\Delta\rho = \langle\rho\rangle - \rho\sqrt{g}$ is the difference in density due to displacing the grids. A detailed description of the analytical formulation can be found in the adaptive particle mesh and moving mesh (MM) hydrodynamics algorithms (Pen 1995, 1998). Eq. 3 can be solved by multi-grid algorithm (Pen 1995, 1998; Zhu et al. 2016b). Then the estimated displacement field is given by

$$\tilde{\mathbf{\Psi}}(\boldsymbol{\xi}) = \nabla\phi(\boldsymbol{\xi}), \tag{4}$$

and the reconstructed density field is given by

$$\delta_R(\boldsymbol{\xi}) = -\nabla\cdot\tilde{\mathbf{\Psi}}(\boldsymbol{\xi}) = -\nabla^2\phi(\boldsymbol{\xi}). \tag{5}$$

3 IMPLEMENTATION AND POWER SPECTRA

We use CUBEP^{3}M (Harnois-Déraps et al. 2013a) to run 140 simulations with a box size of 600 Mpc/h and 512^3 particles. For these simulations, we use cosmological parameters $\Omega_m = 0.321$, $\Omega_\Lambda = 1 - \Omega_m = 0.679$, $h = 0.67$, $\sigma_8 = 0.83$, and $n_s = 0.96$. The initial conditions are computed by transfer function (Lewis et al. 2000) at $z = 100$. Zel'dovich approximation is used to calculate the displacement and initial velocities of particles.

We use the Voronoi tessellation method (van de Weygaert 1994) to estimate the density contrast $\delta_N = \rho/\langle\rho\rangle - 1$ (N stands for nonlinear) from particle distributions, and apply the MM reconstruction to these fields with 512^3 grids. The reconstruction code solves the displacement potentials iteratively until the root mean square (rms) of the results drop from ~ 7.5 to 0.20. The compression limiter is set to be 0.1 (Pen 1995, 1998; Zhu et al. 2016b). For different simulation samples, a different number of iterations are required to get the results of the same rms. A total of 130 simulations converged to the target rms within 2000 iterations, and we use these results for the calculation in this paper. A 2-D projection of one layer of the deformed mesh and the original density field on the mesh are shown in Fig. 1. As expected, the deformed mesh traces the structure very well and the deformed grids do not cross each other, even in the 2-D projection.

We study the Fisher information in the matter power spectra. More generally, the cross power spectrum $P_{\alpha\beta}(k)$ for species α and β ($\alpha = \beta$ for auto power spectrum) is defined as

$$\langle\delta^\dagger_\alpha(\boldsymbol{k})\delta_\beta(\boldsymbol{k}')\rangle = (2\pi)^3 P_{\alpha\beta}(k)\delta_{3\mathrm{D}}(\boldsymbol{k}-\boldsymbol{k}'), \tag{6}$$

where δ_α and δ_β are any two fields and $\delta_{3\mathrm{D}}$ is the three-dimensional Dirac delta function. We typically consider instead the dimensionless power spectrum, $\Delta^2_{\alpha\beta}(k)$, defined as

$$\Delta^2_{\alpha\beta}(k) \equiv \frac{k^3 P_{\alpha\beta}(k)}{2\pi^2}. \tag{7}$$

In the left panel of Fig. 2, we show the matter auto power spectrum of linear theory density fields δ_L, nonlinear density fields (δ_N) from simulations and reconstructed density fields (from Eq. 5). For the simulation results, we use the average value of all 130 simulations and show 1σ standard deviations as error bars.

To quantify the cross-correlation between fields, we compute the cross correlation coefficient $r_{\alpha\beta}(k) \equiv P_{\alpha\beta}/\sqrt{P_{\alpha\alpha}P_{\beta\beta}}$. In the right panel of Fig. 2, we show r_{NL} and r_{RL}. We see that, compared with δ_N, δ_R correlates with δ_L on much wider range of scales. We compare our reconstruction correlation coefficient to that of the E-mode reconstruction, r_{EL}, computed in Yu et al. 2016. Even though r_{RL} decreases from r_{EL} in the nonlinear regime due to the fact that the MM reconstruction cannot recover the shell-crossing present on these scales, we find that linear modes are recovered successfully on scales $k \simeq 0.05 - 0.3$ h/Mpc. Specifically, the scale where $r(k) = 1/2$ increases from $k \simeq 0.2$ h/Mpc to 0.8

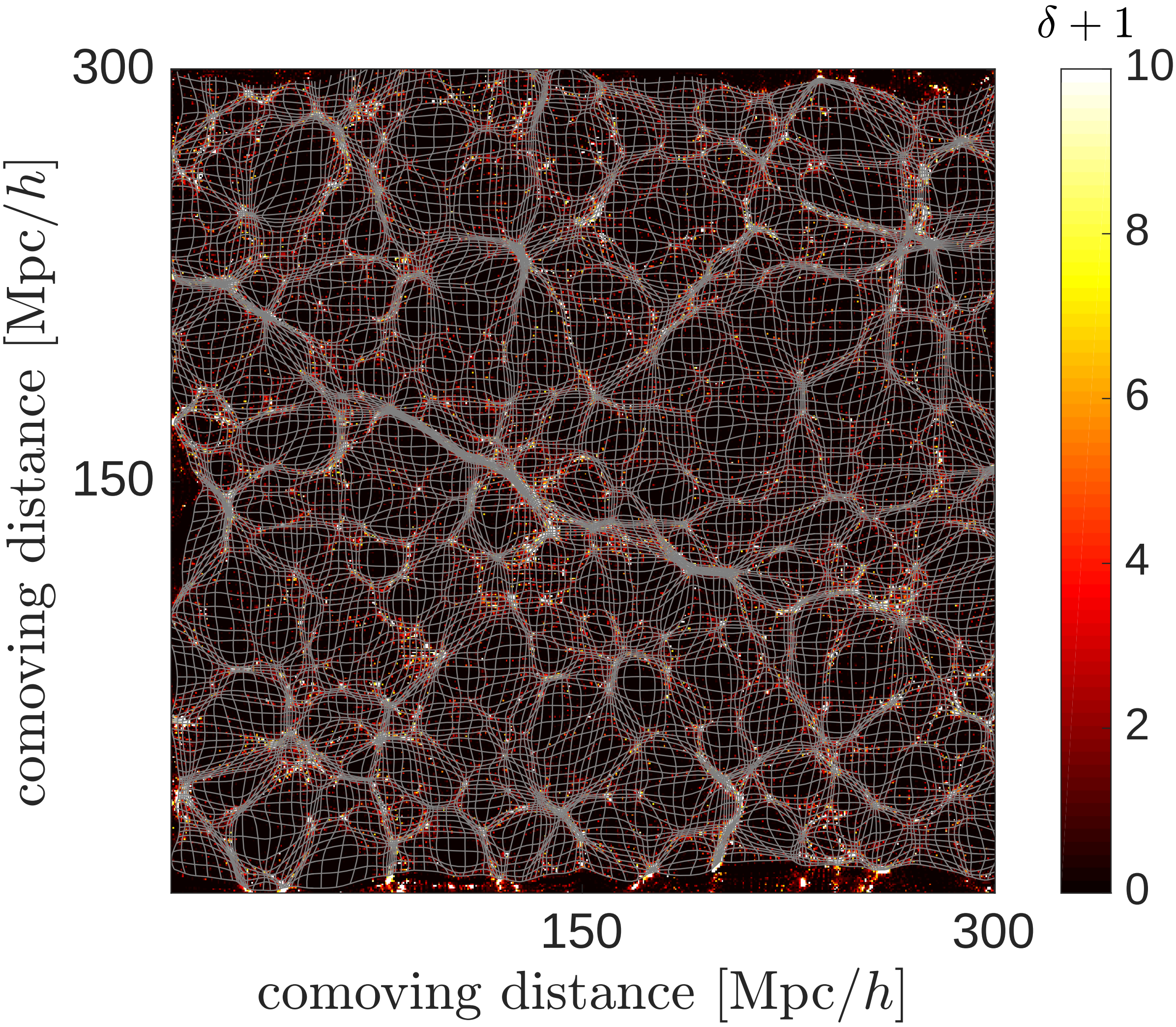

Figure 1. Illustration of MM reconstruction. The 2-D projection of one layer of the deformed mesh of a sample N-body simulation is shown as curved white lines. The density $\rho/\langle\rho\rangle = 1 + \delta$ on the mesh is shown underneath. For clarity, the scale of the density field is cut to 300 Mpc/h, and only every other grid line is plotted.

h/Mpc after reconstruction. In comparison with the results of Zhu et al. (2016b), which showed $r(k \simeq 0.9h/\mathrm{Mpc}) = 1/2$, we find the correlation coefficient falls off at slightly lower wave numbers, which we attribute to using fewer particles per simulation.

4 FISHER INFORMATION CONTENT

Mathamatically, the Fisher information I of the initial scale invariant matter power spectrum, A, is defined as

$$I_A \equiv -\left\langle \frac{\partial^2 \ln \mathcal{L}}{\partial \ln A^2} \right\rangle, \tag{8}$$

where $\mathcal{L}$ is the likelihood (Tegmark et al. 1997). In this paper, the word "information" and the symbol "I" both implicitly mean cumulative Fisher information of A. For Gaussian fields, the likelihood depends on parameters only through the power spectrum $P(k)$, so I can be written as

$$I = -\left\langle \sum_{k,k'} \frac{\partial \ln P(k)}{\partial \ln A} \frac{\partial^2 \ln \mathcal{L}}{\partial \ln P(k) \partial \ln P(k')} \frac{\partial \ln P(k')}{\partial \ln A} \right\rangle, \tag{9}$$

where the angle bracket averages over realizations (Rimes & Hamilton 2005). Eq. 9 can be written in a simpler form in two aspects.

Firstly, we simplify the derivative term $\partial \ln P(k)/\partial \ln A$. For a given density field δ_α, we can conveniently decompose it into a correlated, linear component, and an uncorrelated, noise component with respect to δ_L,

$$\delta_\alpha(k) = r'(k)\delta_L(k) + \delta_n(k), \tag{10}$$

where $\delta_n(k)$ is defined such that the correlation $\langle \delta_L^\dagger(k)\delta_n(k)\rangle = 0$. To solve r', we correlate both sides with δ_L and the uncorrelated noise term drops out,

$$\langle \delta_L^\dagger(k)\delta_\alpha(k)\rangle = r'(k)\langle \delta_L^\dagger(k)\delta_L(k)\rangle. \tag{11}$$

Using the definitions of cross correlation coefficient, $r_{\alpha L}(k) \equiv$

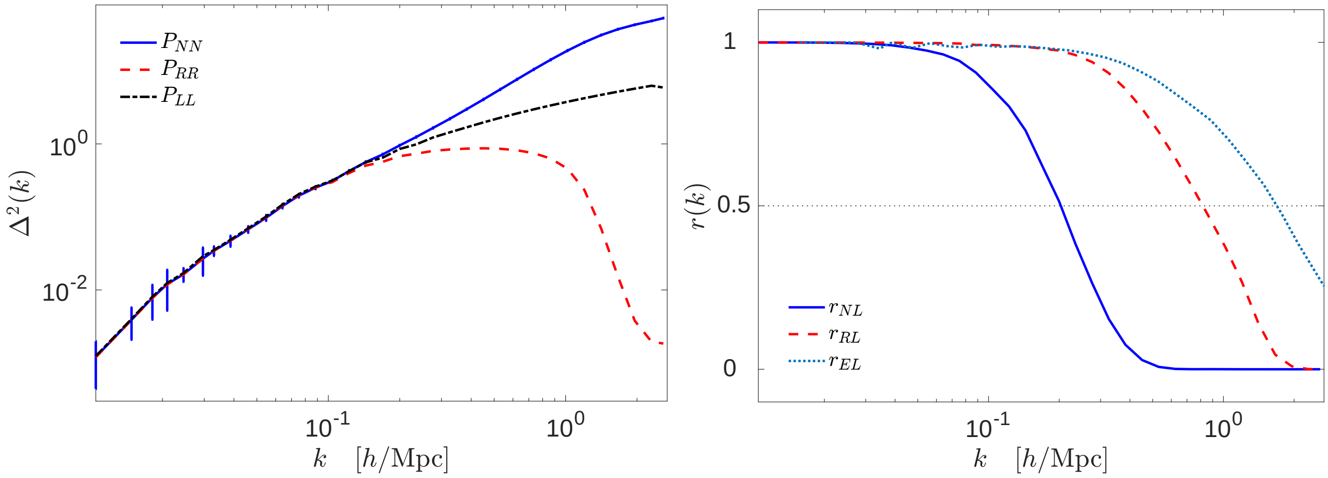

Figure 2. *Left.* The dimensionless power spectrum computed via linear theory (black dash-dotted line), the mean value of 130 N-body simulations with 1σ error bars (blue solid line), and reconstruction of the simulations (red dashed line). *Right.* The cross correlation coefficient between simulation and linear densities r_{NL} (blue solid line), MM reconstructed and linear densities r_{RL} (red dashed line), and E-mode reconstruction r_{EL} (cyan dotted line) from Yu et al. 2016.

$P_{\alpha L}/\sqrt{P_{\alpha\alpha}P_{LL}}$, and bias, $b^2(k) \equiv P_{\alpha\alpha}/P_{LL}$, we can solve for r' as

$$r'(k) = \frac{P_{\alpha L}(k)}{P_{LL}(k)} = r_{\alpha L}(k)b(k). \tag{12}$$

To find the nonlinear term, we square both sides of Eq. 10 and the cross term of the right hand side vanishes,

$$\langle\delta^\dagger_\alpha(k)\delta_\alpha(k)\rangle = r^2_{\alpha L}(k)b^2(k)\langle\delta^\dagger_L(k)\delta_L(k)\rangle + \langle\delta^\dagger_n(k)\delta_n(k)\rangle, \tag{13}$$

and find

$$P_{\alpha\alpha}(k) = r^2_{\alpha L}(k)b^2(k)P_{LL}(k) + P_{nn}(k). \tag{14}$$

With the help of Eq. 12 and Eq. 14, we get

$$\frac{\partial \ln P(k)}{\partial \ln A} = r^2_{\alpha L}(k)b^2(k)\frac{P_{LL}(k)}{P_{\alpha\alpha}(k)} = r^2_{\alpha L}(k). \tag{15}$$

Secondly, we simplify $\partial^2\ln\mathcal{L}/\partial\ln P(k)\partial\ln P(k')$ by using the fact that its expectation value is the Fisher matrix. For Gaussian fields, this is equal to the inverse of the covariance matrix which is diagonal with elements given by the number of modes in each bin (when considering $\boldsymbol{k}$ and $-\boldsymbol{k}$ as the same mode). We can extend this definition to non-Gaussian fields, by taking into account that the covariance matrix is no longer diagonal (Rimes & Hamilton 2005). Thus, we write the Fisher information in terms of matrix multiplication:

$$I(<k_n) = r^2(k)^{\mathrm{T}}\left[\mathrm{C}^{-1}_{\mathrm{norm}}(k,k')\right]_{<k_n} r^2(k'), \tag{16}$$

where

$$\mathrm{C}_{\mathrm{norm}}(k,k') = \frac{\mathrm{Cov}(k,k')}{\langle P(k)\rangle\langle P(k')\rangle} \tag{17}$$

is the normalized covariance matrix, and r is the mean cross correlation of a given density field with δ_L and the subscript $<k_n$ indicates the matrix elements are set to zero for modes $k, k' > k_n$. The covariance matrix is defined as

$$\mathrm{Cov}(k,k') \equiv \frac{\sum_{i,j=1}^{N}\left[P_i(k) - \langle P(k)\rangle\right]\left[P_j(k') - \langle P(k')\rangle\right]}{N-1}, \tag{18}$$

where N is the total number of simulations and angle bracket average these simulations.

The cross-correlation coefficient matrix, or for short the correlation matrix, is defined as

$$\mathrm{Corr}(k,k') = \frac{\mathrm{Cov}(k,k')}{\sqrt{\mathrm{Cov}(k,k)\,\mathrm{Cov}(k',k')}}, \tag{19}$$

representing the correlation between different k modes. The correlation matrices for nonlinear and reconstructed power spectra are shown in the upper-left and lower-right sections of Fig. 3. By definition, the correlation matrix is symmetric with unit diagonal allowing us to overlay the two matrices. For the nonlinear case, it is almost diagonal in the linear regime, $k \lesssim 0.07$ h/Mpc. The off-diagonal elements are produced by strong mode coupling on nonlinear scales and the super-survey tidal effect which is small on linear scales but dominates in the weakly nonlinear regime (Akitsu et al. 2016). The correlation matrix for the nonlinear power spectra has a small amount of negative elements (Corr $\gtrsim -0.18$), which should vanish with more simulations (Takahashi et al. 2009). For the reconstructed correlation matrix, the linear regime extends up to $k \simeq 0.3$ h/Mpc. However, the number and magnitude of negative off-diagonal elements also increases (Corr $\gtrsim -0.49$).

The Fisher information is proportional to the volume. We plot the Fisher information per unit volume of the power spectra of δ_N, δ_L and δ_R in the left panel of Fig. 4. The Fisher information of the linear power spectra is equal to the cumulative number of k-modes, N_k. As expected, Fisher information of δ_N decreases from that of δ_L on scale $k \simeq 0.05$ h/Mpc, and has a flat plateau on small scales, with a saturated value of $I \simeq 2.5\times10^{-5}/(\mathrm{Mpc}/h)^3$, indicating the absence of independent information in the nonlinear regime. In comparison, the information curve of the δ_R power spectra keeps increasing roughly the same as the linear information until $k \simeq 0.3$ h/Mpc, and reaches a value of $I \simeq 1.3\times10^{-3}/(\mathrm{Mpc}/h)^3$ at $k \simeq 2.7$ h/Mpc, a factor of 50 times greater than I_{δ_N}. As an example to illustrate its strength, we compare the Fisher information given by the MM reconstruction method with the logarithmic density mapping method (Neyrinck et al. 2009). We find that MM reconstruction gives over 10 times more

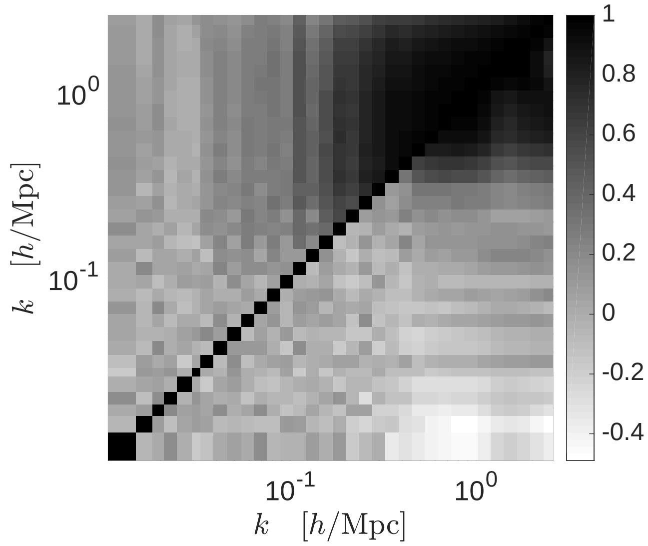

Figure 3. The correlation matrix from 130 nonlinear power spectra (the upper triangular elements) and reconstructed power spectra (the lower triangular elements).

information. It also appears to perform significantly better than the standard BAO reconstruction using the Zel'dovich approximation (Ngan et al. 2012), although a direct comparison is left for future work.

To test the upper limit of information that the MM reconstruction can recover, we also checked the Fisher information given by δ_E (Yu et al. 2016) as a reference, which indicates the maximum possible information available via reconstruction procedures. We find that I_{δ_E} is 3 times higher ($150 I_{\delta_N}$) than MM reconstruction. This gives motivation to continue to develop and optimize our reconstruction algorithms to achieve this theoretical target.

In some previous works, the cross correlation r^2 terms have been set to unity in Eq. 16, which artificially increases the information. To demonstrate this, we plot this case in the right panel of Fig. 4. We see that neglecting r^2 causes there to be an artificial increase in information on small scales ($k \gtrsim 1 h$/Mpc). We also see that the information of the logarithmic density mapping is much higher than it is in the left panel. Including the correlation coefficient ensures that the information we compute is that present in the initial conditions and not spuriously induced by the transformation procedure. This therefore resolves the problems discussed in Harnois-Déraps et al.'s (2013b) section "Information about what?" We conclude that, in the context of BAO analysis and extracting other primordial cosmological parameters, we should take into account the correlation term r^2 and use Eq. 16 to compute the Fisher information.

Another way to quantify the nonlinear scale of δ_α is via the information plateau's linear equivalent scale, k_p, satisfying

$$I_{\delta_L}(k_p) = I_{\delta_\alpha}(k \to \infty). \tag{20}$$

In the left panel of Fig. 4, we can see that k_p is just the scale on which the horizontal dotted line crosses I_{δ_L} curve. Practically, we use I_{δ_α} ($k = 2.7\ h$/Mpc) as a proxy of $I_{\delta_\alpha}(k \to \infty)$, where k is large enough such that $r \to 0$, ensuring the convergence, or saturation of I_{δ_α}. We find that for δ_N, $k_p \simeq 0.15$ h/Mpc. The MM reconstruction increases k_p to 0.4 h/Mpc, whereas the logarithmic density mapping method only increases it to 0.19 h/Mpc.

5 CONCLUSION

We study the Moving-Mesh algorithm's ability to estimate the underlying displacement field and reconstruct the linear density fields using 130 cosmological N-body simulations. We measure the power spectra and the associated covariance of the nonlinear density fields, and the reconstructed density fields. We quantify the result by (i) cross-correlating them with the linear density fields, (ii) studying the k-mode coupling in the correlation matrix, and (iii) computing the cumulative Fisher information contained in these power spectra. We also compared with the E-mode reconstruction and logarithmic density mapping Gaussianization techniques. We find that Moving-Mesh method gives better results than previous works (e.g. Neyrinck et al. 2009; Zhang et al. 2011; Harnois-Déraps et al. 2013b), and on scales relevant to the BAO, our result approaches the optimal E-mode reconstruction. The advantage of this method is that it doesn't include cosmological dynamics and thus no cosmological assumptions are required. Future steps include quantifying halo Poisson noise and bias contamination from realistic measurements, and determining the quantitative impact on BAO and RSD measurements.

ACKNOWLEDGEMENTS

We thank Xin Wang and Kwan Chuen Chan for friendly and helpful discussions. We thank Hong-Ming Zhu for discussions and detailed comments and feedback on drafts of this work. We thank Yu Yu for discussions and providing an optimized version of the reconstruction code. Computations were performed on the General Purpose Cluster supercomputer at the SciNet HPC Consortium. SciNet is funded by: the Canadian Foundation for Innovation under the auspices of Compute Canada; the Government of Ontario; Ontario Research Fund - Research Excellence; and the University of Toronto.

REFERENCES

Akitsu K., Takada M., Li Y., 2016, preprint (arXiv:1611.04723)
Eisenstein D. J., Seo H.-J., Sirko E., Spergel D. N., 2007a, ApJ, 664, 675
Eisenstein D. J., Seo H.-J., Sirko E., Spergel D. N., 2007b, ApJ, 664, 675
Harnois-Déraps J., Pen U.-L., Iliev I. T., Merz H., Emberson J. D., Desjacques V., 2013a, MNRAS, 436, 540
Harnois-Déraps J., Yu H.-R., Zhang T.-J., Pen U.-L., 2013b, MNRAS, 436, 759
Lewis A., Challinor A., Lasenby A., 2000, ApJ, 538, 473
Meiksin A., White M., 1999, MNRAS, 308, 1179
Neyrinck M. C., Szapudi I., Szalay A. S., 2009, ApJ, 698, L90
Ngan W., Harnois-Déraps J., Pen U.-L., McDonald P., MacDonald I., 2012, MNRAS, 419, 2949
Pen U.-L., 1995, ApJS, 100, 269
Pen U.-L., 1998, ApJS, 115, 19

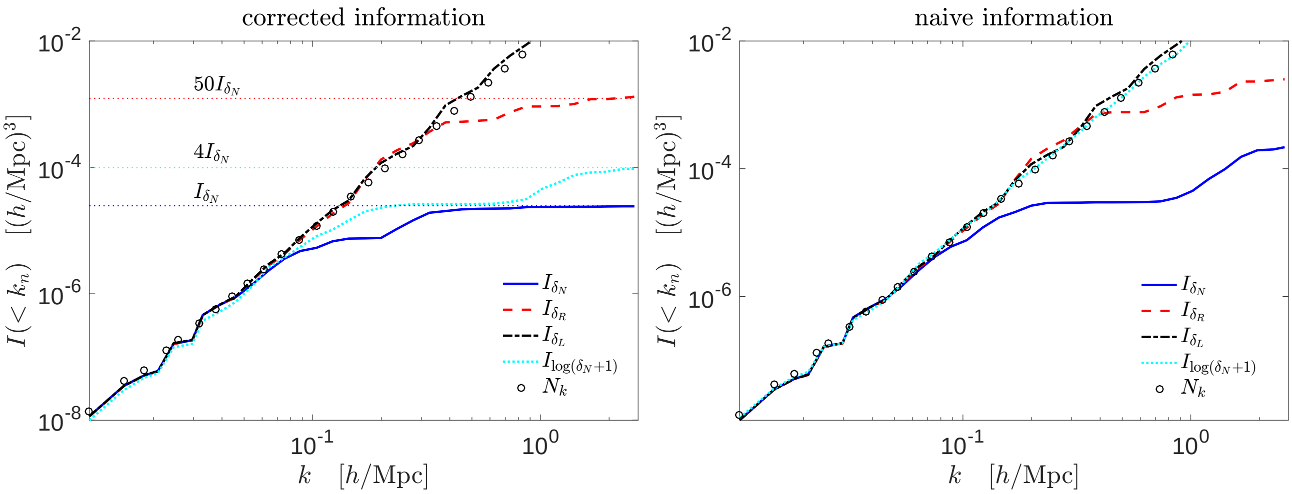

Figure 4. *Left.* The Fisher information (thick curves) per unit volume as a function of wave number. The blue solid, red dashed, and black dash-dotted curves correspond to the power spectra of δ_N, δ_R and δ_L respectively, and the cyan dotted curve corresponds to the logarithmic density mapping. The circles are the cumulative number of k modes. Thin dotted horizontal lines indicate the value of the Fisher information at $k \simeq 2.7$ h/Mpc. *Right.* Same as the left panel except setting $r \equiv 1$ in Eq. 16. The black dash-dotted, blue solid, and cyan dotted curves match the results in Rimes & Hamilton 2005; Neyrinck et al. 2009. This naive estimate does not account for the lack of correlation of the final density field with the initial conditions, and represents an overestimate of the information.

Rimes C. D., Hamilton A. J. S., 2005, MNRAS, 360, L82
Takahashi R., et al., 2009, ApJ, 700, 479
Tegmark M., Taylor A. N., Heavens A. F., 1997, ApJ, 480, 22
Weinberg D. H., 1992, MNRAS, 254, 315
Yu H.-R., Harnois-Déraps J., Zhang T.-J., Pen U.-L., 2012, MNRAS, 421, 832
Yu H.-R., Pen U.-L., Zhu H.-M., 2016, preprint (arXiv:1610.07112)
Zel'dovich Y. B., 1970, A&A, 5, 84
Zhang T.-J., Yu H.-R., Harnois-Déraps J., MacDonald I., Pen U.-L., 2011, ApJ, 728, 35
Zhu H.-M., Yu Y., Pen U.-L., Chen X., Yu H.-R., 2016b, preprint (arXiv:1611.09638)
Zhu H.-M., Pen U.-L., Chen X., 2016a, preprint (arXiv:1609.07041)
van de Weygaert R., 1994, A&A, 283, 361

This paper has been typeset from a TEX/LATEX file prepared by the author.